

On-line Tracking of Fuel Cell System Impedance Using Extended Kalman Filter

Andrej Debenjak^{*,a}, Matej Gašperin^{a,b}, Janko Petrovčič^{a,c}

^aJožef Stefan Institute, Jamova 39, 1000 Ljubljana, Slovenia

^bUniversity of West Bohemia, Faculty of Electrical Engineering, RICE, Univerzitni 26, 306 14 Pilsen, Czech Republic

^cCentre of Excellence for Low-carbon Technologies – CO NOT, Hajdrihova 19, 1000 Ljubljana, Slovenia
andrej.debenjak@ijs.si

This paper presents a new measurement equipment and computational method for on-line estimation and tracking of PEM fuel cell system impedance. The algorithm is developed to address one of the main issues influencing the reliability and durability of PEM fuel cell technology – the water management in fuel cell stacks, namely fuel cell flooding and membrane drying. Using the appropriate model formulation and system state variables, the model allows direct estimation of the characteristic values of the fuel cell impedance at different frequencies and thus avoids the need for transformation of the measured signals to the frequency domain. Estimation of the model state variables is performed with Extended Kalman filter, which is renowned for its computational efficiency, while the probabilistic interpretation of the algorithm ensures adequate management of the uncertainties. The performance of the diagnostic system is explored on experimental data from a commercial fuel cell stack consisting of 80 fuel cells.

1. Introduction

Proton Exchange Membrane (PEM) fuel cells (FC) experience reliability issues due to water management faults (Li et al., 2008). On the one hand, when produced water is not effectively removed from the cell, flooding of gas-diffusion layer occurs, while excessive water removal leads to membrane drying, on the other hand. Both faults negatively affect the performance of PEM fuel cells, and therefore have to be properly handled in order to ensure long-term reliability of PEM fuel cell operation (Schmittinger and Vahidi, 2008).

Design solutions for eliminating cell flooding and membrane drying from occurring (i.e. humidifiers, complex PEM materials, gas-channels design) are mostly prohibitively expensive for commercial applications and contribute to system complexity. Therefore, a better approach is to use diagnostics tools to detect the fault and to utilize the information in the control system to eliminate it.

In this paper, Electrochemical Impedance Spectroscopy (EIS) is used as a diagnostic tool. The EIS has already been proven as effective diagnostic tool on laboratory-scale FC systems (Yuan et al., 2007). Fouquet et al. (2006) used the EIS for parameter estimation of proposed FC model and showed the possibility of distinguishing nominal operating cell from flooded or dried. Additionally, Onanena et al. (2011) showed that the method is appropriate for estimation of aging time. Le Canut et al. (2006) performed EIS based diagnostics on a stack similar to the one used in study presented in this paper. The authors reported they can detect cell flooding and membrane drying, and also anode catalyst carbon monoxide poisoning. Despite good diagnostics performance, the measurement equipment used in those studies is prohibitively expensive for commercial applications. More recently, Wasterlain et al. (2011) built up a high-voltage impedance spectrometer for testing multi-cell FC stacks. The spectrometer exhibits great performance specifications and gives good results, but at the expense of high costs, unsuited for commercial applications. Furthermore, Steiner et al. (2011) used wavelet packet transform to diagnose fuel cell flooding based only on voltage signal. Although the EIS has been widely explored, it still suffers from disadvantages, which are connected with expensive equipment and complex computation. The

problem even escalates when the method is to be implemented to a commercial FC stack consisted of few tens of cells.

This paper investigates an alternative hardware and software implementation of the EIS based diagnostics of FC systems. It addresses previously stressed disadvantages of existing solutions for water faults diagnostics by employing only market-acceptable solutions. It presents an in-house developed measurement system, and a new method for on-line estimation of FC impedance. The main capability of the developed system is precise measuring of voltage of individual cell inside a stack. Further, the impedance of the cell is computed with Extended Kalman filter (EKF) algorithm, which ensures the same diagnostic capabilities as standard processing methods with less processor time consumed. The testing of the proposed implementation was performed on a commercial FC system consisted of 80 PEM FCs.

2. Fuel Cell Voltage Monitor

When it comes to commercially oriented applications, the measurement equipment needs to be capable of measuring voltages of all individual cells inside a kW-range stack of FCs, rather than measuring only a single cell or a stack of few cells in the case of laboratory testing (Miller and Bazylak, 2011). State-of-the-art laboratory equipment and data acquisition boards can successfully cope with the measurement requirements, but their design solutions and measurement concepts are not appropriate for commercial applications, primarily because of high costs. Additionally, target requirements regarding reliability, size, and weight for such commercial equipment are much stricter than for the laboratory-grade one (Webb and Møller-Holst, 2001). To fulfil the requirements, the manufacturers use design solutions that measure joint voltage of two or even more adjacent cells with rather low resolution (Vale et al., 2005).

The developed Fuel Cell Voltage Monitor (FCVM), presented in Figure 1, overrides earlier discussed shortcomings of nowadays measurement solutions for commercial applications. In its essence, the FCVM is a low-cost general-purpose device, designed for accurate measurement of voltage signals of FC stack consisted of up to 90 FCs.

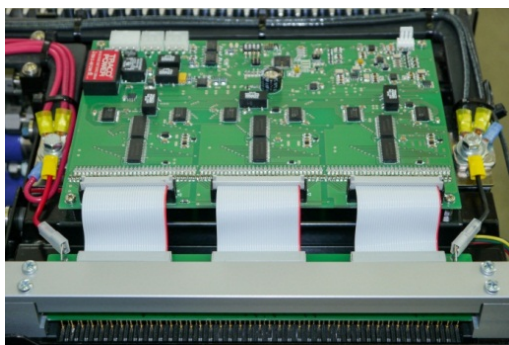


Figure 1: The FCVM connected to a commercial fuel cell stack

The main problem with measuring individual cell voltage inside a large stack is mainly connected with common-mode (C-M) voltage potential, which is the origin of high complexity and costs of the laboratory-grade equipment. Typically, commercial PEM FC stacks embody 50 to 100 cells resulting in open-circuit voltage of 60 to 120 V. Such high C-M potential prohibits usage of integrated-circuit multiplexors in a standard way. To override this limitation, the FCVM's analog input stage for the cell voltages is designed around three pairs of multiplexors, each coupled with a differential amplifier, which reject C-M voltage and change the differential signals to ground referenced single-ended ones in order to fit to the AD converter.

The main feature of the FCVM is the ability to perform measurements intended for more complex diagnostics tools. The EIS based diagnostics relies on precise measurements of FC voltage and current, which must exhibit high resolution, and must be carried out at high sampling rate. Both, high resolution and sampling rate are required because of the superimposed AC voltage signals, which are to be measured, and their low amplitude not higher than few millivolts and frequencies ranging up to few hundred Hertz. As such, the FCVM provides the means for EIS diagnostics. It enables measuring changes in voltage of specific FC inside a stack with resolution of $\sim 80 \mu\text{V}$ at high sampling rate. More precisely, the FCVM enables simultaneous measurements of three cells voltages at sampling rate of 5 kHz. Beside the individual cells voltages, voltage and current of the complete stack are also measured at the same sampling rate, and with a resolution of $\sim 24 \text{ mV}$ and $\sim 10 \text{ mA}$, respectively. To measure all 90 cells, the measurements are performed in interlaced manner in 30 consecutive time periods.

Besides providing the measurement capacities, the FCVM was built to be on-line EIS-based diagnostic module with its own computation resources provided by on-board ARM Cortex M3 based microcontroller.

3. EKF based algorithm for impedance estimation

In order to enable on-board computation of individual cell impedance with FCVM with limited storage and computational resources, an alternative computational method for on-line tracking of cell impedance has been developed. The proposed algorithm is based on application of Bayesian filtering theory and results in a recursive estimation algorithm.

The impedance is defined as a ratio of the voltage phasor to the electric current phasor. To estimate its value, given two sampled waveforms, one usually computes the phasors in frequency domain and the impedance is given by their ratio. In the specific case of FC impedance estimation, there are some important properties that are often ignored (Adzakpa et al., 2008) (i) in case of sinusoidal current excitation, the voltage will have the same sinusoidal form corrupted by random noise, (ii) the signals (both voltage and electric current) contain only one frequency component, (iii) the frequency of the component is known and is the same for both signals. Taking into account the above, we can model both signals as:

$$i(t) = I \cdot \cos(\omega t + \phi_i) + e_i(t), \quad (1)$$

$$u(t) = U \cdot \cos(\omega t + \phi_u) + e_u(t), \quad (2)$$

where we can ignore the DC component of the signals without the loss of generality. Assuming known frequency ω , both signals are fully specified by their amplitude and phase. The complex phasors are:

$$\mathbf{I} = I e^{j\phi_i}, \quad (3)$$

$$\mathbf{U} = U e^{j\phi_u}. \quad (4)$$

And finally the complex impedance is defined by their ratio:

$$\mathbf{Z} = \frac{\mathbf{U}}{\mathbf{I}} = \frac{1}{U} e^{j(\phi_i - \phi_u)}. \quad (5)$$

It is important to note, that given this representation, the only quantities required are the amplitudes (I, U) and phase angles (ϕ_i, ϕ_u). However, equally important in the estimation procedure is a proper management of the noise components in Eq. (1) and (2). For automatic estimation of the signals, we describe the time evolution of the parameters with a state-space model. A general non-linear discrete-time state-space model with additive noise has the following form:

$$\mathbf{x}_k = f(\mathbf{x}_{k-1}) + \mathbf{v}_k, \quad (6)$$

$$\mathbf{y}_k = g(\mathbf{x}_k) + \mathbf{e}_k, \quad (7)$$

where k is sample index, \mathbf{x}_k is the hidden system state, \mathbf{y}_k is the model output, $f(\cdot)$ and $g(\cdot)$ are nonlinear functions and \mathbf{v}_k and \mathbf{e}_k are random variables with known stochastic properties. The state-space model of a sinusoidal waveform can be constructed in different ways. In this implementation, the hidden system states are the amplitude and phase $\mathbf{x}_k = (I, \phi_i)^T$ and the output is the sinusoidal waveform Eq. (8).

$$y_k = I \cdot \cos\left(\frac{\omega k}{f_s} + \phi_i\right) + e_k = \mathbf{x}_k(1) \cdot \cos\left(\frac{\omega k}{f_s} + \mathbf{x}_k(2)\right) + e_k, \quad (8)$$

where the dynamical model of the unknown parameters is random walk. With proper selection of system states and assuming a time-invariant and known frequency ω , the presented equations can model any sinusoidal waveform without a DC component. The DC component can either be removed in pre-processing or included in the model. For the sake of clarity we will assume that all the signals are without a DC component.

The derivation and final shape of the model for voltage signal is exactly the same as for electric current and will be skipped for the sake of brevity. Both models can later be merged into one model with 4 states and two outputs.

3.1 Bayesian state estimation and the Extended Kalman filter

The task of estimation can be interpreted as a problem of inference of a discrete-time stochastic process:

$$\mathbf{y}_k \sim p(\mathbf{y}_k | \mathbf{x}_k), \quad (9)$$

$$\mathbf{x}_k \sim p(\mathbf{x}_k | \mathbf{x}_{k-1}). \quad (10)$$

Here, \mathbf{x}_k is a vector known as the state variable, y_k are the observations, and $p(\cdot | \cdot)$ denotes the conditional probability density of the variable. By Bayesian state estimation we mean the recursive evaluation of the filtering distribution, $p(\mathbf{x}_k | \mathbf{y}_{1:k})$, using Bayes rule (Simon, 2006):

$$p(\mathbf{x}_k | \mathbf{y}_{1:k}) = \frac{p(y_k | \mathbf{x}_k) p(\mathbf{x}_k | \mathbf{y}_{1:k-1})}{p(y_k | \mathbf{y}_{1:k-1})}, \quad (11)$$

$$p(\mathbf{x}_k | \mathbf{y}_{1:t-1}) = \int p(\mathbf{x}_k | \mathbf{x}_{k-1}) p(\mathbf{x}_{k-1} | \mathbf{y}_{1:k-1}) d\mathbf{x}_{k-1}, \quad (12)$$

where $\mathbf{y}_{1:k} = (y_1, y_2, \dots, y_k)$ denotes the set of all observations. The integration in (12) is over the whole support of the involved probability density functions. Eq. (11) and (12) are analytically traceable only for a limited set of models. The most notable example of a traceable model is linear Gaussian model for which (11) and (12) are equivalent to the Kalman filter. For other models, operations Eq. (11) and (12) do not yield posterior density in the form of a Gaussian and they need to be evaluated approximately. One possible method is the Extended Kalman filter, where the probability densities in (9) and (10) are:

$$p(\mathbf{x}_k | \mathbf{x}_{k-1}) = \mathcal{N}(f(\mathbf{x}_{k-1}), \mathbf{Q}), \quad (13)$$

$$p(y_k | \mathbf{x}_k) = \mathcal{N}(g(\mathbf{x}_k), \mathbf{R}), \quad (14)$$

where $f(\cdot)$ and $g(\cdot)$ are vector functions of appropriate dimensions, $\mathcal{N}(\mu, \mathbf{R})$ denotes Gaussian probability density with mean value μ and variance \mathbf{R} . Using Taylor expansion at the current point estimate as follows:

$$p(\mathbf{x}_k | \mathbf{x}_{k-1}, \mathbf{y}_{1:k-1}) \approx \mathcal{N}(f(\hat{\mathbf{x}}_{k-1}), \mathbf{P}_t), \quad (15)$$

$$p(\mathbf{x}_k | \mathbf{x}_{k-1}, \mathbf{y}_{1:k}) \approx \mathcal{N}(f(\hat{\mathbf{x}}_{k-1}) - \mathbf{K}(y_k - g(\hat{\mathbf{x}}_{k-1})), \mathbf{P}_{t|t}), \quad (16)$$

where \mathbf{K} and \mathbf{P}_t are the Kalman gain and posterior covariance matrix from the Kalman filter.

$$\mathbf{S} = \mathbf{C}^T \mathbf{P}_{t-1} \mathbf{C} + \mathbf{R} \quad (17a)$$

$$\mathbf{K} = \mathbf{P}_{t-1} \mathbf{C} \mathbf{S}^{-1} \quad (17b)$$

$$\mathbf{P}_{t|t} = \mathbf{P}_{t-1} - \mathbf{P}_{t-1} \mathbf{C}^T \mathbf{S}^{-1} \mathbf{C} \mathbf{P}_{t-1} \quad (17c)$$

$$\mathbf{P}_t = \mathbf{A} \mathbf{P}_{t|t} \mathbf{A}^T + \mathbf{Q} \quad (17d)$$

Where $\mathbf{A} = \frac{d}{dx_k} f(\mathbf{x}_k)$ and $\mathbf{C} = \frac{d}{dx_k} g(\mathbf{x}_k)$ (Simon, 2006). This approximation is performed in each step.

3.2. EKF based algorithm for FCS impedance tracking

The applied algorithm for impedance tracking in FCS was designed by implementing the presented solutions in the final version of the algorithm. A single iteration of the estimation algorithm for a single cell in the stack is summarized in Table 1.

Table 1: EKF based algorithm for impedance estimation

Algorithm: On-line tracking of FCS impedance with EKF	
1.	Start with initial estimates of voltage and current waveforms $I_0, \phi_{i,0}, U_0, \phi_{u,0}$ and set the sampling frequency f_s
2.	for k=1:N
3.	Collect new samples of $u(k)$ and $i(k)$
4.	Compute the EKF estimate of states I_k and $\phi_{i,k}$ (17)
5.	Compute the EKF estimate of states U_k and $\phi_{u,k}$ (17)
6.	Compute the FCS impedance Z_k (5)
7.	end for

The key advantages of the algorithm, namely the proper management of uncertainty and recursive implementation, are both inherited from the EKF. Another desired property is, that the impedance is not assumed to be constant (as opposed to FFT-based implementations, where non-stationary signals actually cripple the estimation) and the algorithm recursively estimates its current value. Finally, the EKF retains the low computational complexity of the linear Kalman filter, which makes it an appropriate choice for advanced applications of diagnostic tools in FCS (i.e. on-board monitoring of individual cell impedance).

4. Experimental setup and measurements

The measurement setup consisted of a commercial 8.5 kW PEM fuel cell power unit, electronic load, FCVM measuring system, and desktop computer. The unit was connected to an electronic load, which

served as a load and to provide the power unit with excitation current. The FCVM and desktop computer formed the data acquisition subsystem of the measurement setup. The FCVM was performing measurements, whereas the desktop computer was used to control the experiment.

Based on the previous research (Debenjak et al., 2013), it was decided to observe the impedance of the cells at three frequencies, i.e. 10, 30 and 100 Hz. During the measurement, the current's DC component was set to 40 A, and the amplitude of the sinusoidal current excitation at all four frequencies was set to 1 A. The AC component is 5 % of the DC component and is therefore small enough not to cause problems due to non-linearity of the cells.

To achieve different fault scenarios, the power unit was fed with air at different moisture content in order to provoke flooding and drying inside the stack. In the first time period, the power unit operated on normal ambient air. In this case, the air parameters at the fuel cell inlet were; temperature $\sim 50^{\circ}\text{C}$ and relative humidity $\sim 12\%$. Next, the power unit was fed with dry air in order to provoke membrane drying inside the cells. The parameters of inlet air were; temperature $\sim 50^{\circ}\text{C}$ and relative humidity below 4%. Further, extremely moist air was applied, which resulted in flooding of the fuel cells. The parameters were; temperature $\sim 50^{\circ}\text{C}$ and relative humidity 100%. Finally, the power unit again operated under normal conditions.

5. Results of EKF impedance tracking

The on-line tracking of the cell impedance is achieved with implementation of the Extended Kalman filter algorithm, given in Table 1. The results of the estimation for a single cell at 10Hz and sampling frequency of 500Hz are given in Figures 2 and 3. The left part of the images shows the tracking of the waveform parameters in terms of mean (bold) and confidence interval (shaded), and the right part shows the estimated impedance value, where the size of the marker corresponds to the uncertainty interval. It can be seen that the algorithm converges in a few periods of the signal (1 period equals 50 samples) and the confidence interval of the estimate narrows down considerably.

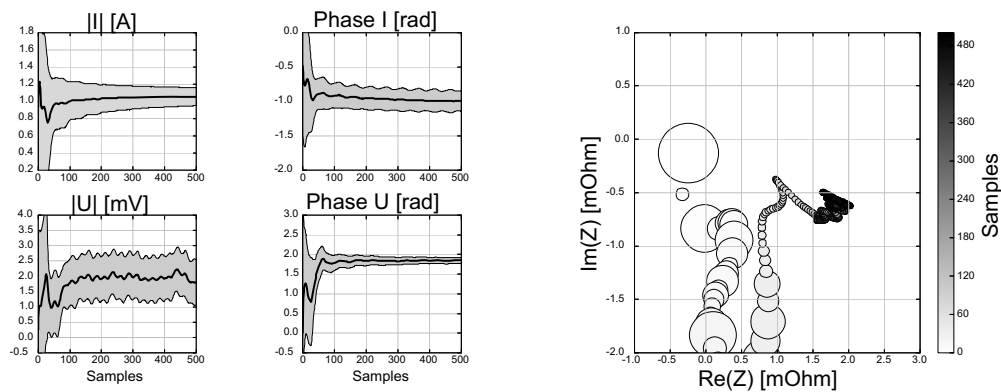


Figure 2: Estimates of the electric current and voltage signals (left) and cell impedance (right), computed at 10 Hz signal frequency and 500 Hz sampling frequency using 500 samples and normal cell operation

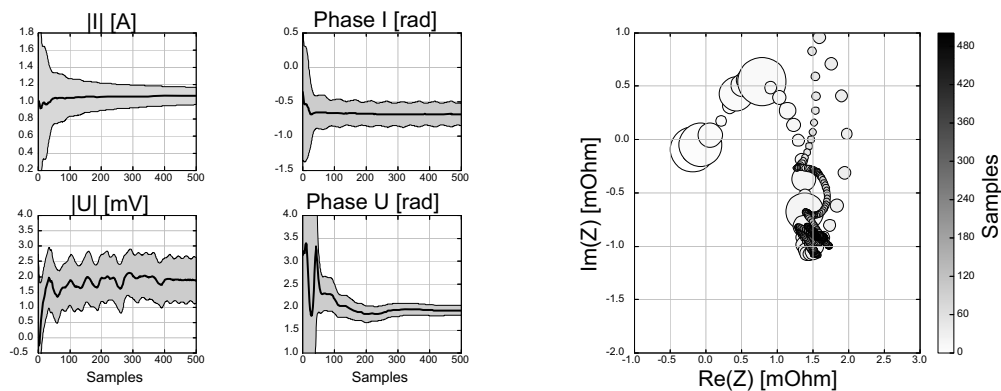


Figure 3: Estimates of the electric current and voltage signals (left) and cell impedance (right), computed at 10 Hz signal frequency and 500 Hz sampling frequency using 500 samples and flooded cell

The final impedance estimates from all the scenarios and different frequencies are summarized in Table 2. The results are given in terms of mean value and a very conservative 95 % confidence interval. It can be seen, that the algorithm is accurate enough to distinguish between the different scenarios.

Table 2: The EKF algorithm estimates of FCS impedance

	10Hz		30Hz		100Hz	
	$\Re(\mathbf{Z})[m\Omega]$	$\Im(\mathbf{Z})[m\Omega]$	$\Re(\mathbf{Z})[m\Omega]$	$\Im(\mathbf{Z})[m\Omega]$	$\Re(\mathbf{Z})[m\Omega]$	$\Im(\mathbf{Z})[m\Omega]$
Normal	1.64 ± 0.36	-0.49 ± 0.25	1.12 ± 0.36	-0.51 ± 0.26	0.59 ± 0.15	-0.39 ± 0.29
Dry	1.95 ± 0.35	-0.67 ± 0.30	1.13 ± 0.34	-0.57 ± 0.24	0.45 ± 0.22	-0.16 ± 0.23
Flooded	1.50 ± 0.40	-0.88 ± 0.32	0.96 ± 0.32	-0.55 ± 0.24	0.30 ± 0.28	-0.03 ± 0.18

6. Discussion

The results indicate that successful on-board EIS based diagnostics of FCS can be achieved using appropriate measurement equipment and optimized computational procedure. The distinctive properties of the presented prototype are monitoring and diagnostics of individual cell in the stack and the innovative on-board algorithm for impedance estimation. The results confirm the main idea that the impedance can be computed from on-line estimates of the waveform parameters. This implementation is computationally efficient as the computation involves simple matrix operations, fully recursive and can properly manage the noise components in the measurements.

The FCVM and its algorithm are currently still in the prototype development phase. The algorithm estimates are extremely conservative and therefore exhibit a high uncertainty. To properly tune the algorithm performance, further testing and experimenting is required.

Acknowledgement

The authors thank the Centre of Excellence for Low-carbon Technologies – CO NOT, financed by the Slovenian Ministry of Higher Education, Science and Technology and co-financed by the European Regional Development Fund and the project EXLIZ – CZ.1.07/2.3.00/30.0013, which is co-financed by the European Social Fund and the state budget of the Czech Republic for their financial support.

References

- Adzakpa K.P., Agbossou K., Dube Y., Dostie M., Fournier M., Poulin A., 2008, PEM Fuel Cells Modeling and Analysis Through Current and Voltage Transient Behaviors, *IEEE Transactions on Energy Conversion*, 23(2), 581-591.
- Debenjak A., Gašperin M., Pregelj B., Atanasijević-Kunc M., Petrovčič J., Jovan V., 2013, Detection of flooding and drying inside a PEM fuel cell stack, *SV - Journal of Mechanical Engineering*, 59(1), 56-64.
- Fouquet N., Doulet C., Nouillant C., Dauphin-Tanguy G., Ould-Bouamama B., 2006, Model based PEM fuel cell state-of-health monitoring via ac impedance measurements, *Journal of Power Sources*, 159(2), 905-913.
- Le Canut J.M., Abouatallah R.M., Harrington D.A., 2006, Detection of Membrane Drying, Fuel Cell Flooding, and Anode Catalyst Poisoning on PEMFC Stacks by Electrochemical Impedance Spectroscopy, *Journal of The Electrochemical Society*, 153(5), A857-A864.
- Li H., Tang Y., Wang Z., Shi Z., Wu S., Song D., Zhang J., Fatih K., Zhang J., Wang H., Liu Z., Abouatallah R., Mazza A., 2008, A review of water flooding issues in the proton exchange membrane fuel cell, *Journal of Power Sources*, 178(1), 103-117.
- Onanena R., Oukhellou L., Candusso D., Harel F., Hissel D., Aknin P., 2011, Fuel cells static and dynamic characterizations as tools for the estimation of their ageing time, *International Journal of Hydrogen Energy*, 36(2), 1730–1739.
- Schmittinger W., Vahidi A., 2008, A review of the main parameters influencing long-term performance and durability of PEM fuel cells, *Journal of Power Sources*, 180(1), 1-14.
- Simon D., 2006, *Optimal State Estimation*, John Wiley & Sons, Hoboken, New Jersey.
- Steiner N.Y., Hissel D., Moçotéguy P., Candusso D., 2011, Non-intrusive diagnosis of polymer electrolyte fuel cells by wavelet packet transform, *International Journal of Hydrogen Energy*, 36(1), 740-746.
- Vale M., Epp B., Masse B., Joos N.I., 2005, Fuel Cell Voltage Monitoring System and Associated Electrical Connectors, US Patent, no. US2005/0215124.
- Wasterlain S., Candusso D., Harel F., Hissel D., François X., 2011, Development of new test instruments and protocols for the diagnostic of fuel cell stacks, *Journal of Power Sources*, 196(12), 5325-5333.
- Yuan X., Wang H., Sun J.C., Zhang J., 2007, AC impedance technique in PEM fuel cell diagnosis – A review, *International Journal of Hydrogen Energy*, 32(17), 4365-4380.